JOURNAL OF AIRCRAFT
Vol. 41, No. 4, July–August 2004

Application of System Identification Techniques to the F-111C and PC 9/A Aircraft

Jan S. Drobik* and Geoffrey J. Brian†
Defence Science and Technology Organisation, Fishermans Bend, Victoria, Australia, 3207

An overview of some past and recent uses of system identification techniques to generate flight dynamic model databases for flight simulators is presented. Two cases are examined, the first being the F-111C, in which the adaptive flight control system can mask the aircraft damped responses, thus making system identification difficult. In the second case, a conventional turboprop trainer, the PC 9/A aircraft, with strong power effects was examined. The techniques used included both equation and output error techniques. Although extensive flight test programs were carried out, it was found that substantial ground-based estimation was also required to provide adequate angle of attack variation and insight into various phenomena such as power effects. The flight data were not sufficient to determine comprehensively the aircraft's characteristics across the envelope in all dependent variable dimensions. The system identification techniques are significant because they are the main source of the dynamic derivatives. As a result, the system identification technique derived databases were used to augment and validate more extensive wind-tunnel data for use in flight simulator models.

Nomenclature

A_Y, A_Z	=	body-axes linear accelerations
a	=	gradient of line of best fit
b	=	intercept of line of best fit
C_{lp}	=	rolling moment due to roll rate
$C_{l\beta}$	=	rolling moment due to sideslip
C_{mq}	=	pitching moment due to pitch rate
$C_{m\alpha}$	=	pitching moment due to angle of attack
$C_{m\delta e}$	=	pitching moment due to elevator deflection
$C_{N\alpha}$	=	normal force due angle of attack
C_{nr}	=	yawing moment due to yaw rate
$C_{n\beta}$	=	yawing moment due to sideslip
$C_{n\delta r}$	=	yawing moment due to rudder deflection
$C_{Y\beta}$	=	side force due to sideslip
$C_{Y\delta r}$	=	side force due to rudder deflection
H	=	altitude
K_α, K_β	=	angle of attack, sideslip scale factor
M	=	Mach number
p, q, r	=	angular roll, pitch, yaw rates
α, β	=	angle of attack, sideslip
δ_a	=	equivalent aileron deflection
δ_e	=	elevator deflection
δ_H	=	horizontal stabilator deflection
δ_r	=	rudder deflection
ε	=	error
Λ	=	wing sweep
ϕ, θ	=	roll, pitch angle

Introduction

THE use of system identification techniques to generate aircraft stability and control derivatives has found broad usage in the aerospace community. The literature tends to be dominated by the application of these techniques for unique aircraft configurations, for example, X-29 (Ref. 1) and X-31 (Ref. 2), at a few points of interest. The literature is sparser when system identification techniques applied to the full flight envelope of unconventional, or even conventional aircraft, are considered.

In this paper, results from two flight-test programs spanning two decades of Defence Science and Technology Organisation (DSTO) (formerly known as Aeronautical Research Laboratory) research, using system identification techniques, will be presented. In the first case, the application of these techniques, for predata processing and aerodynamic characterization, will be described for the variable-geometry General Dynamics F-111C aircraft. The subsequent blending of the results with a broader incremental wind-tunnel database will be examined. The second example will cover the development of a flight dynamic model for the Pilatus PC 9/A turboprop trainer aircraft that uses wind-tunnel, datasheet, and computational fluid dynamics (CFD) data augmented with aerodynamic parameters obtained from system identification techniques. In both cases, flight-test data were also used to validate the models.

Application to the F-111C Aircraft

In 1987, a flight-test program was undertaken to characterize the aerodynamics of the F-111C aircraft throughout its operational envelope (Fig. 1). The variable geometry F-111C aircraft flight envelope covers the subsonic flight regime through to approximately Mach 2 (Fig. 2). System identification techniques were used to characterize the stability and control derivatives across the envelope, and the data were used to adjust an extensive incremental wind-tunnel data set. In many cases, significant shifts to the data were required to provide a validated database across the full flight spectrum.

Adaptive Flight Control System

The F-111C's adaptive flight control system masks the aircraft's natural response. As a result, the aerodynamic characterization is made more difficult when system identification techniques are used, due to the reduction in parameter identifiability. The yaw control system uses a fixed gain, whereas in the roll and pitch control systems, the gains depend on the system state. The roll and pitch systems use an adaptive control strategy to maintain the same aircraft flying characteristics over a wide range of operating conditions, that is, to minimize aircraft handling differences at various speeds, altitudes, and wing-sweep angles. In each of the roll and pitch control systems, the feedback transfer function exhibits a closed-loop mode called the adaptive mode, with a frequency in the range of 2–3 Hz,

Received 7 September 2003; revision received 4 December 2003; accepted for publication 6 December 2003.

*Principal Research Scientist, Flight Systems Branch, Air Vehicles Division, 506 Lorimer Street; jan.drobik@dsto.defence.gov.au. Senior Member AIAA.

†Senior Aeronautical Engineer, Flight Systems Branch, Air Vehicles Division, 506 Lorimer Street; geoff.brian@dsto.defence.gov.au.

Fig. 1 General Dynamics F-111C variable geometry strike aircraft fitted with air data probe.

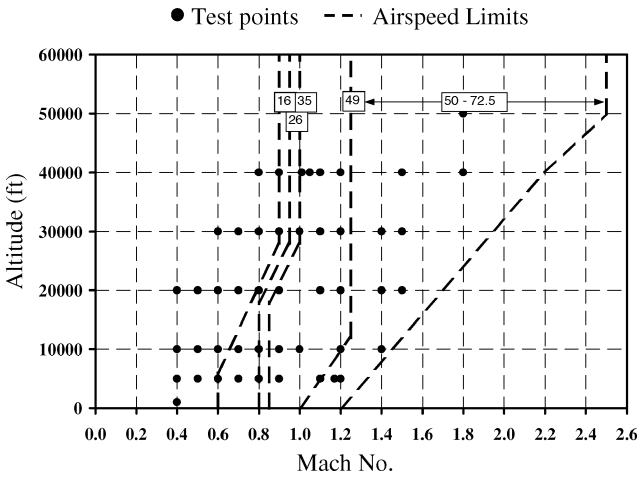

Fig. 2 F-111C flight envelope with flight test points, Λ = 16–72.5 deg.

and a relative damping that varies inversely with gain. For any given flight condition, the system gain is adjusted to be as high as possible, consistent with maintenance of an adaptive mode relative damping ratio. As a result, the natural damping of the airframe is masked because the adaptive flight-control aims for a damping ratio of 0.3 over the flight envelope.

During the flight-test program, this problem was overcome, to some extent, by application of appropriate rapid stick inputs during the maneuver. Additionally, pumping the control stick before the maneuver increased the system gains. Another difficulty was in obtaining consistent and repeatable control inputs because these techniques had preceded test pilot training curricula of the time.

Earlier system identification work at NASA Dryden Flight Research Center using output-error techniques[3,4] also indicated substantial difficulties in the aerodynamic characterization of the F-111, resulting, among other things, from control system interaction.

Data Compatibility

The flight-test program was conducted in two phases. The first phase used the onboard computer air data system (CADS) for air data, whereas the second phase also made use of a nose boom transducing unit (NBTU) for dedicated air data measurements. To reduce flight-test time and to minimize data issues, a number of flight data postprocessing programs were developed. The main area of investigation was in the development of flight-path reconstruction software. This is a nonlinear estimation problem used to obtain accurate flight-path data from noisy biased measurements. The method made use of extended Kalman filterlike nonlinear estimation algorithms.[5] A range of instrument biases and scale factors, K_α and K_β, were obtained, and these were essential because the air data were uncorrected for positional errors. In the case of the CADS, the sideslip vane errors were shown to be substantial.

Results from data collected by the CADS and NBTU indicated that the CADS had adequate dynamic characteristics, albeit with an average scale error of approximately 0.94 (under reading) for angle of attack and 1.5–1.6 (over reading) for angle of sideslip for the case shown (Fig. 3). The NBTU scale factors for the alpha vane were of similar magnitude (1.06), but over reading, whereas the sideslip scale factor was reduced to 1.1 (over reading). The improvement in

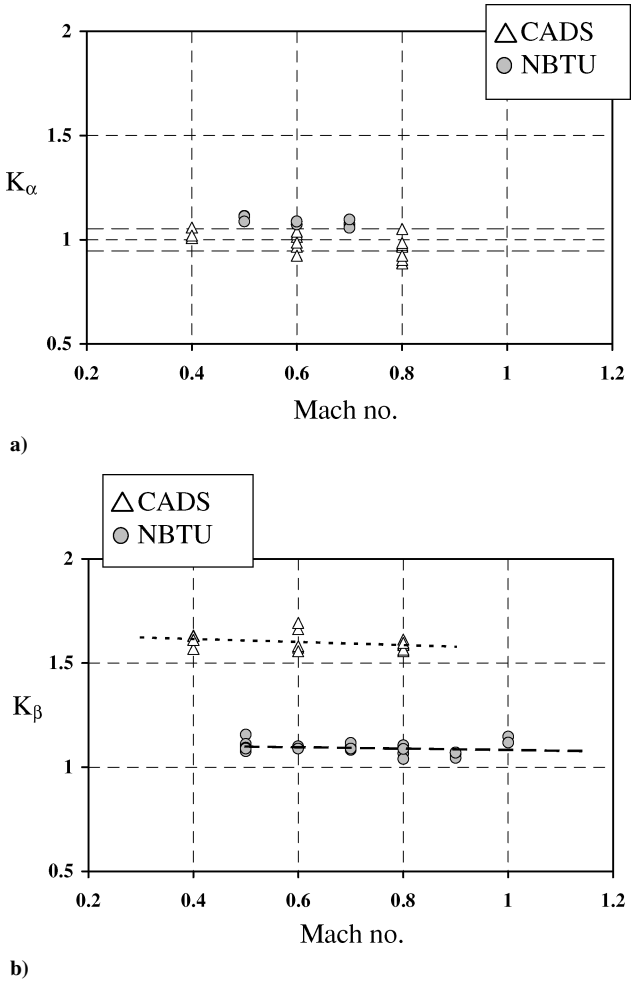

Fig. 3 Scale factors: a) angle of attack and b) angle of sideslip, Λ = 35 deg.

sideslip reading was due to the NBTU vane position being located well forward of the fuselage local flowfield. In comparison, the CADS sideslip vane is mounted on the underside of the fuselage centerline.

The K_α was important in resolving trim angle of attack and establishing a reference for comparisons with wind-tunnel, data, given the 1-deg wing–body angle-of-attack offset. However, the variation in the scale factors was approximately 10%. In the case of the angle-of-attack vane, the parameter identification results indicated a relative insensitivity to the small K_α values. In the case of the CADS angle of sideslip vane, the variation was overwhelmed by the large-scale factor (50–60% over reading).

The use of data compatibility techniques and the use of both standard aircraft instruments, that is, CADS and crew module accelerometers, along with dedicated flight-test instrumentation, allowed for minimal disruption to the flight-test program due to typical instrumentation issues.

Aerodynamic Estimation

Aerodynamic characterization of the F-111C aircraft was achieved by the use of the output-error system identification technique program pEst.[6] An interactive parameter estimation program, pEst, solves a vector set of time-varying, ordinary differential equations of motion. The program estimates a set of aerodynamic stability and control derivatives that minimize an error cost function based on the weighted difference between the model's computed response and the measured response. The Cramer–Rao bounds give an approximation to the variance of the results and, as Maine and Iliff indicated, a factor of 10 was applied to the calculated bounds to take into account the flight-test noise coloring compared to the theoretical assumption of white noise.[7]

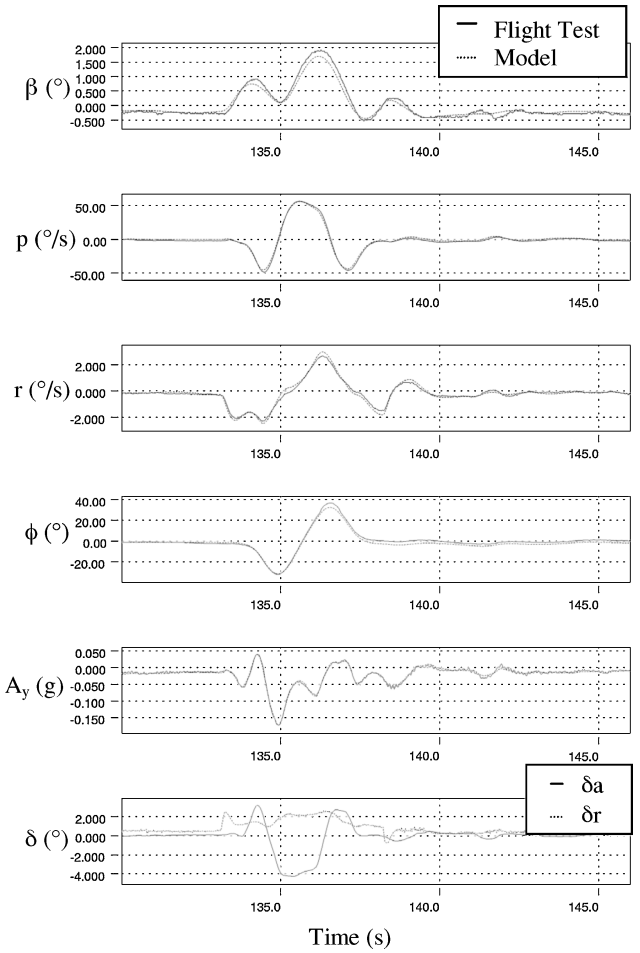

Fig. 4 Lateral flight test response and pEst comparison: $\Lambda = 50$ deg, $M = 1.1$, $h = 20{,}000$ ft.

Figure 4 compares the model results from pEst with flight-measured responses for a typical lateral maneuver. In general, the matches were good. For some flight-test conditions, the inability to switch off the adaptive flight-control system led to difficulties in generating control inputs that resulted in the aircraft's natural response not being overwhelmed by the control system damping as mentioned earlier.

Flight Simulator Data Development

Flight-test data were collected throughout the F-111's operating envelope; however, these represented discrete flight conditions. The data were not sufficient to determine the aircraft's characteristics comprehensively across the envelope in all dependent variable dimensions, such as the aerodynamic variation with angle of attack, angle of sideslip, altitude, and Mach number. In addition, significant scatter was observed in the aerodynamic parameters for similar flight conditions. In Fig. 5, the weathercock stability derivative $C_{n\beta}$ is shown against Mach number. The results show the limited flight data available and the scatter.

Wind-tunnel aerodynamic data provided by General Dynamics were used to supplement and smooth the flight-test aerodynamic data. The aim was to maintain the trend shown in the wind-tunnel data while the magnitude was adjusted to be representative of the flight-test data.

Flight-identified aerodynamic coefficients and derivatives were adjusted to be representative of the wind-tunnel reference location and then compared with their wind-tunnel equivalent over a range of angles of attack for discrete Mach numbers and altitudes. The differences between these data, ε, were calculated for each aerodynamic parameter. A straight line of best fit was computed for the difference values and then applied to the wind-tunnel-derived

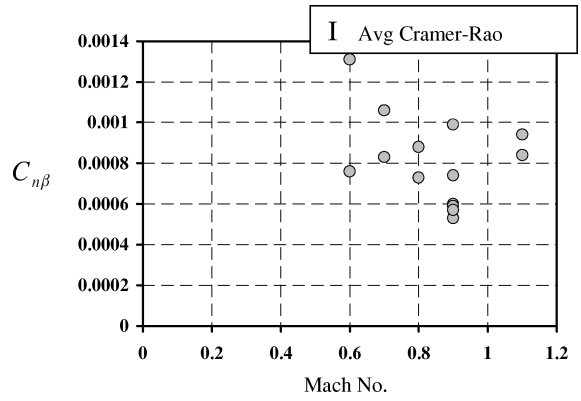

Fig. 5 Estimated $C_{n\beta}$: $\Lambda = 45$ deg and $h = 20{,}000$ ft.

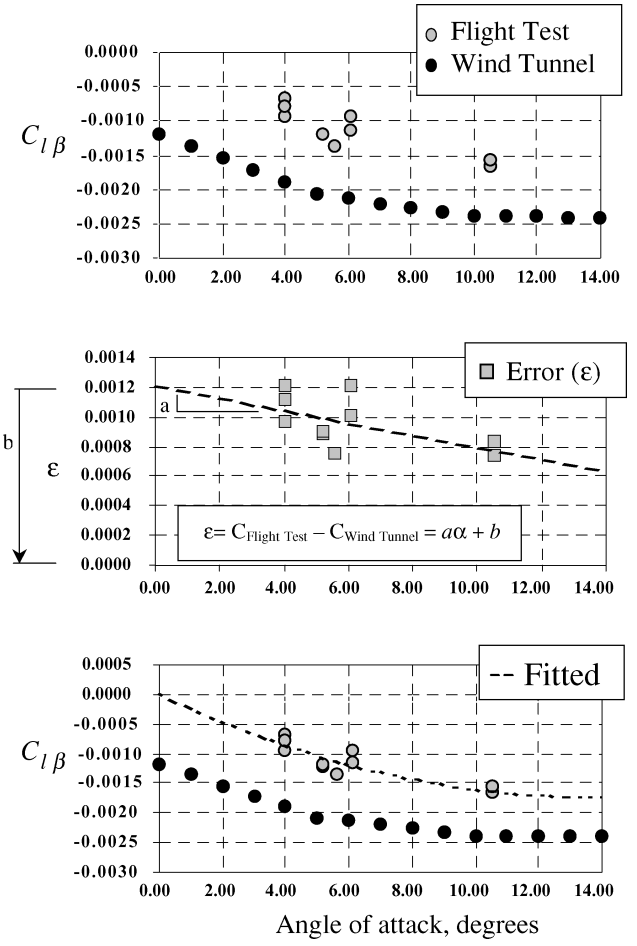

Fig. 6 $C_{l\beta}$ vs angle of attack: a indicates error equation gradient and b indicates the error equation intercept.

data. This adjustment resulted in the wind-tunnel data matching the magnitude of the flight-identified data while the trend shown in the more extensive wind-tunnel data set was maintained and the scatter smoothed as well. This procedure is illustrated in Fig. 6 for the rolling moment due to sideslip derivative $C_{l\beta}$.

The technique described is one of several developed. This technique was found to be unsuitable for a number of aerodynamic parameters at particular flight conditions because of the choice of a linear error equation and insufficient flight data. The linear error equation effectively translated (b) and modified the gradient (a) of the wind-tunnel trendline. The latter effect occasionally resulted in a modified trend line having steep, or shallow, inappropriate gradients, as illustrated in Fig. 7 for the roll damping derivative C_{lp}. This

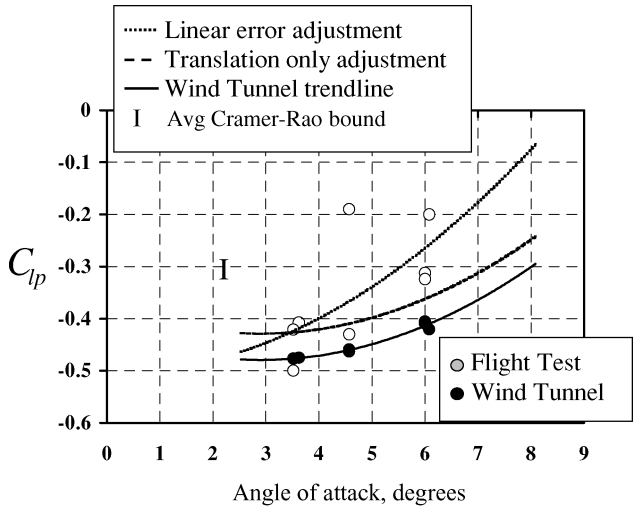

Fig. 7 Example of poor adjustment of C_{lp} by the use of a linear error equation: $\Lambda = 26$ deg and $M = 0.8$.

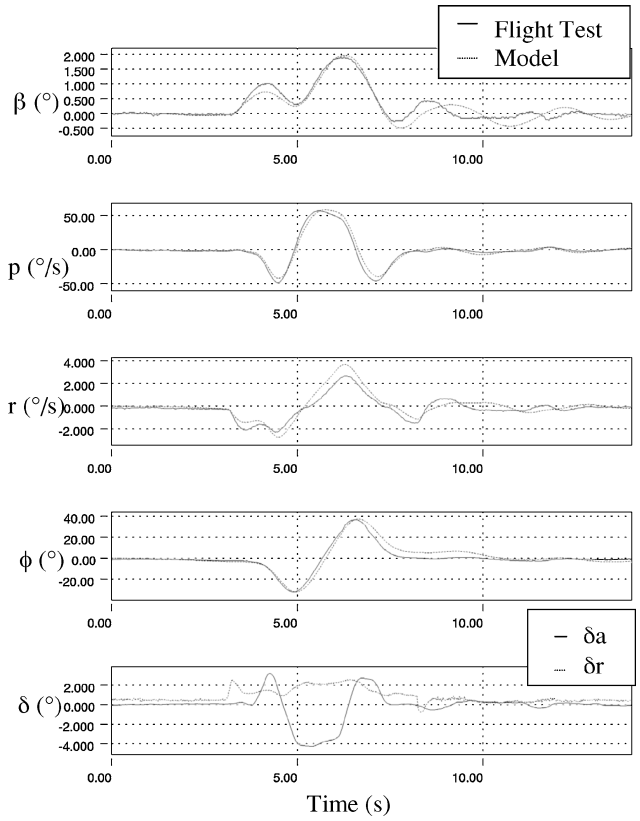

Fig. 8 Lateral flight-test response and model comparison: $\Lambda = 50$ deg, $M = 1.1$, and $h = 20{,}000$ ft.

was overcome to some extent by the application of only a translation to the wind-tunnel trend when flight data were sparse, or nonlinear error equations when necessary.

The adjustment procedure provided a dataset that was at times less than satisfactory at some flight conditions, but acceptable across the flight envelope; ultimately the technique is an engineering solution to a necessarily limited set of flight-test data points.

Comparisons of the aircraft's response computed with the DSTO F-111C flight dynamic model for a lateral and a longitudinal doublet maneuver are presented in Figs. 8 and 9. The angle of sideslip and yaw rate reconstructions do not match the measured responses as well as the pEst estimation in Fig. 4. However, they were deemed to be within an acceptable limit for pilot simulation activities. The flight dynamic model was developed before the widespread

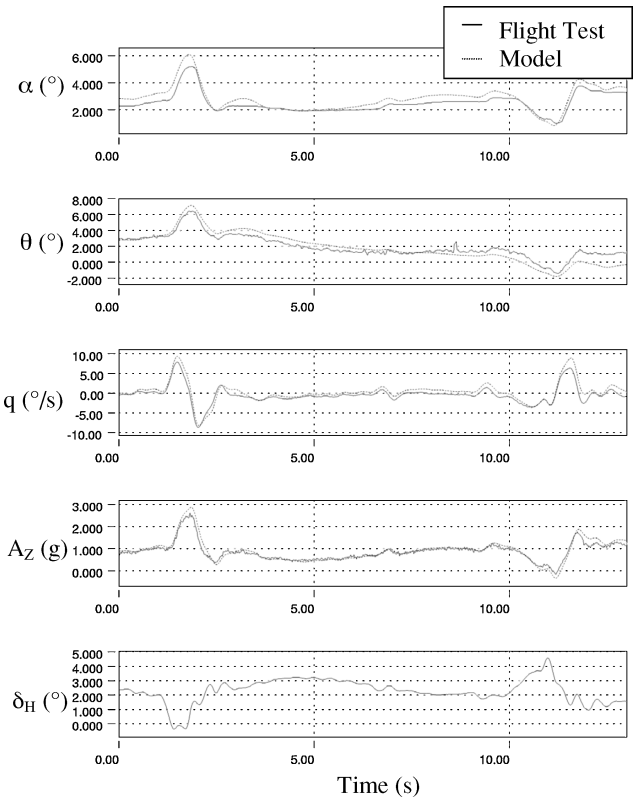

Fig. 9 Longitudinal flight-test response and model comparison, $\Lambda = 72.5$ deg, $M = 1.1$, and $h = 5000$ ft.

Fig. 10 Pilatus PC9/A turboprop trainer aircraft.

adoption of civil (Federal Aviation Administration, International Civil Aircraft Organisation[8] and International Airline Transport Association[9]) or military simulator standards and the issue of acceptability would be worth revisiting.

Application to PC 9/A Aircraft

The Pilatus PC 9/A is a military turboprop trainer aircraft (Fig. 10). A flight-test program was conducted in 1998 and 1999 to establish aerodynamic loads over the full operational flight spectrum for use in a full-scale fatigue test. An extensive wind-tunnel test and CFD program was developed to support the loads work.[10] The test program also provided an opportunity to investigate propeller power effects to aid the development of a flight dynamic model.[11] Propeller power effects had been seen as a significant handling problem with aircraft such as the North American Mustang in World War II.[12]

Again, system identification techniques were applied to estimate the aircraft's aerodynamic properties from the flight data. In this case, an equation-error technique using stepwise regression (SWR) software written in MATLAB® was applied, in addition to the

output-error analyses using the program pEst. As expected, the PC 9/A aircraft analyses did not provide significant difficulties given the simple manual flight control and conventional configuration layout.[13,14] However, there were a number of results that proved counterintuitive in the powered approach and landing configurations, as well as when the aircraft air brake[15] was deployed. A selection of these results, together with the differences in offsets between various system identification techniques are examined in following sections.

Conventional Configuration

The flight-derived aerodynamic derivative data were compared with wind-tunnel results and data sheet sources. The latter aerodynamic data was estimated with Digital DATCOM[16,17] and sourced from Pilatus. Figure 11 shows the results for three lateral parameters, namely, the side force due to sideslip derivative $C_{Y\beta}$, the weathercock derivative $C_{n\beta}$, and the rolling moment due to sideslip derivative $C_{l\beta}$, over the flight-test angle-of-attack range.

The results for the lateral derivatives show good agreement, as expected, between the output-error and equation-error techniques. Similar agreement was found when compared with the wind-tunnel and empirical results. The Cramer–Rao bounds of the pEst results increase at the higher angles of attack, indicating increased uncertainty; however, the bounds were still comparatively small. For clarity, only the average Cramer–Rao bounds are shown in Fig. 11.

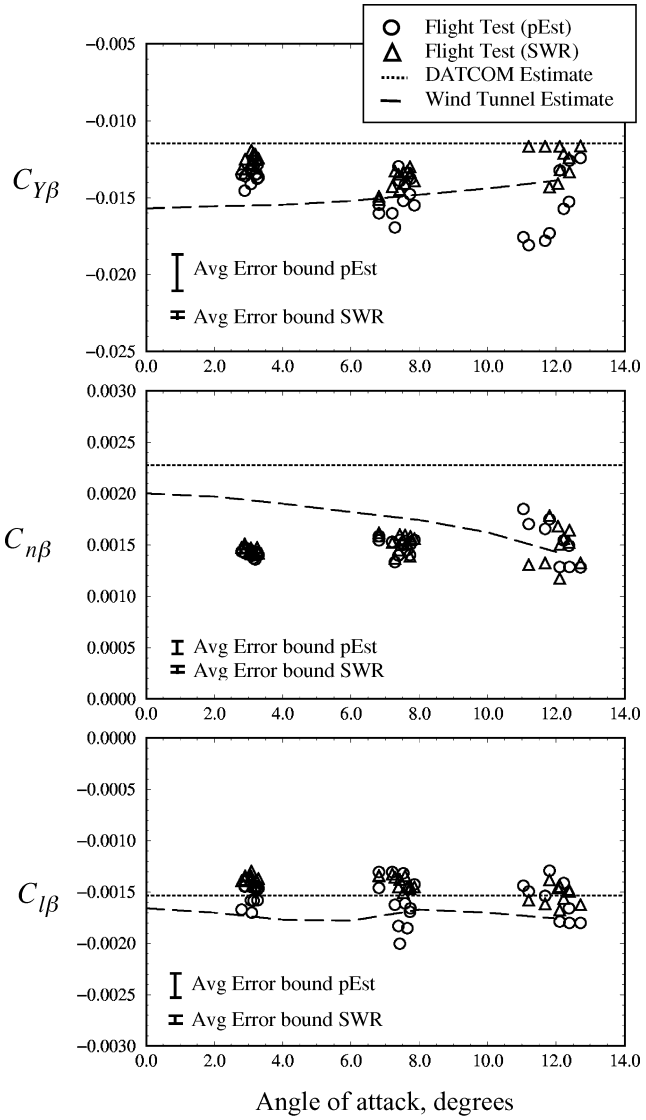

Fig. 11 PC 9/A lateral derivative flight estimates compared with wind-tunnel and DATCOM data.

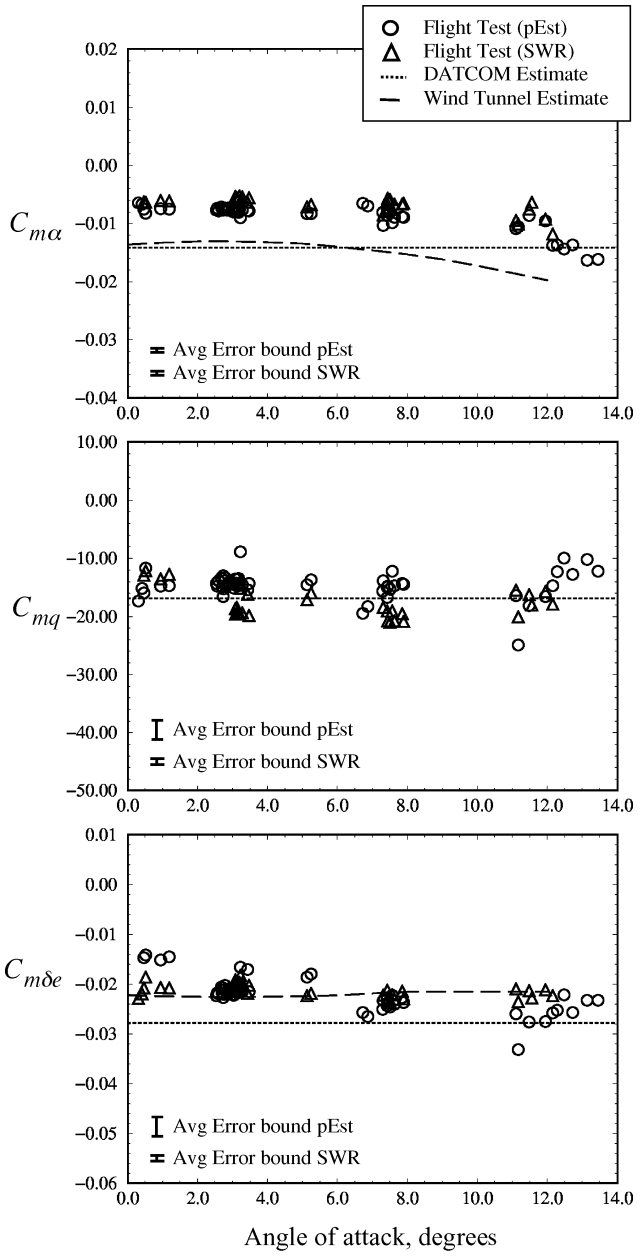

Fig. 12 PC 9/A longitudinal derivative flight estimates compared with wind-tunnel and DATCOM data.

Figure 12 illustrates similar results for three longitudinal parameters, the pitch stiffness derivative $C_{m\alpha}$, the pitch damping derivative C_{mq}, and the pitch moment due to elevator deflection derivative $C_{m\delta e}$.

The results for the longitudinal derivatives show good agreement between both system identification techniques. The agreement of the flight-test data with the wind-tunnel and DATCOM estimates were reasonable, given that these data represent the power-off condition only. This is due to the unavailability of the power-on data at the time of writing. The exception is $C_{m\alpha}$, which was generally smaller than both the wind-tunnel and empirical estimates. It is hypothesized that the difference is due to the two competing effects of the increased dynamic pressure and the reduced angle of incidence imbalance acting on the portion of the horizontal tail within the propeller slipstream. The reduction in angle of incidence dominates, resulting in an overall reduction in the pitch stiffness.

Air Brake Deployed Configuration

The effect of air brake deployment on the aircraft aerodynamics was assessed with a limited number of longitudinal and lateral

doublet maneuvers. The air brake was mounted on the centerline of the underside of the fuselage approximately aft of the wing trailing edge. The hinge pivot line was aligned with the flap hinge line. The test points were performed at 5000 and 15,000 ft, and the results were similar. As a result, for the database development the values were averaged. No wind-tunnel data were available for comparison.

The air brake was expected to provide incremental additions to the pitching moment and axial force coefficients, with minimal impact on the other derivatives. The system identification results (Table 1) showed increases in magnitude of the pitch damping and pitch control derivatives. However, the results also showed increases in magnitude of the normal force due to angle-of-attack derivative and a decrease in magnitude of the pitch stiffness when compared with the conventional configuration data.

Changes to the lateral stability derivatives were of particular interest. It is hypothesised that there was an increase in magnitude of $C_{Y\beta}$ resulting from the increase in the aircraft's side area when yawed with the air brake deployed. An increase in $C_{n\beta}$ followed because the air brake is located aft of the air craft's center of gravity, and, therefore, the side force produced a restoring moment. A reduction in the yaw damping was also evident and resulted from the disturbed airflow emanating from the air brake influencing the flow over the ventral fin. The most interesting lateral change was a reduction in the side force control derivative. However, the rudder control power was unchanged. This result suggests that whereas the side force for a given rudder deflection is reduced, the unchanged moment it produces about the aircraft center of gravity is not an intuitive result.[15] An investigation of these hypotheses is proposed, with a combined CFD and wind-tunnel program.

Table 1 Averaged aerodynamic derivatives: clean configuration compared with the air brake deployed

Derivative	Clean aircraft	pEst	pEst, % change	SWR	SWR, % change
$C_{N\alpha}$	$8.53E-2$	$9.23E-2$	8.21	$8.59E-2$	0.70
$C_{m\alpha}$	$-6.53E-3$	$-6.28E-3$	−3.83	$-4.92E-3$	−24.66
C_{mq}	$-1.53E+1$	$-1.57E+1$	2.61	$-1.95E+1$	27.45
$C_{m\delta e}$	$-1.93E-2$	$-2.18E-2$	12.95	$-2.02E-2$	4.66
$C_{Y\beta}$	$-1.32E-2$	$-1.65E-2$	25.00	$-1.52E-2$	15.15
$C_{n\beta}$	$1.44E-3$	$1.68E-3$	16.67	$1.94E-3$	34.72
C_{nr}	$-2.11E-1$	$-1.68E-1$	−20.38	$-2.03E-1$	−3.79
$C_{Y\delta r}$	$3.38E-3$	$2.03E-3$	−39.94	$1.72E-3$	−49.11
$C_{n\delta r}$	$-1.91E-3$	$-1.81E-3$	−5.24	$-1.90E-3$	−0.52

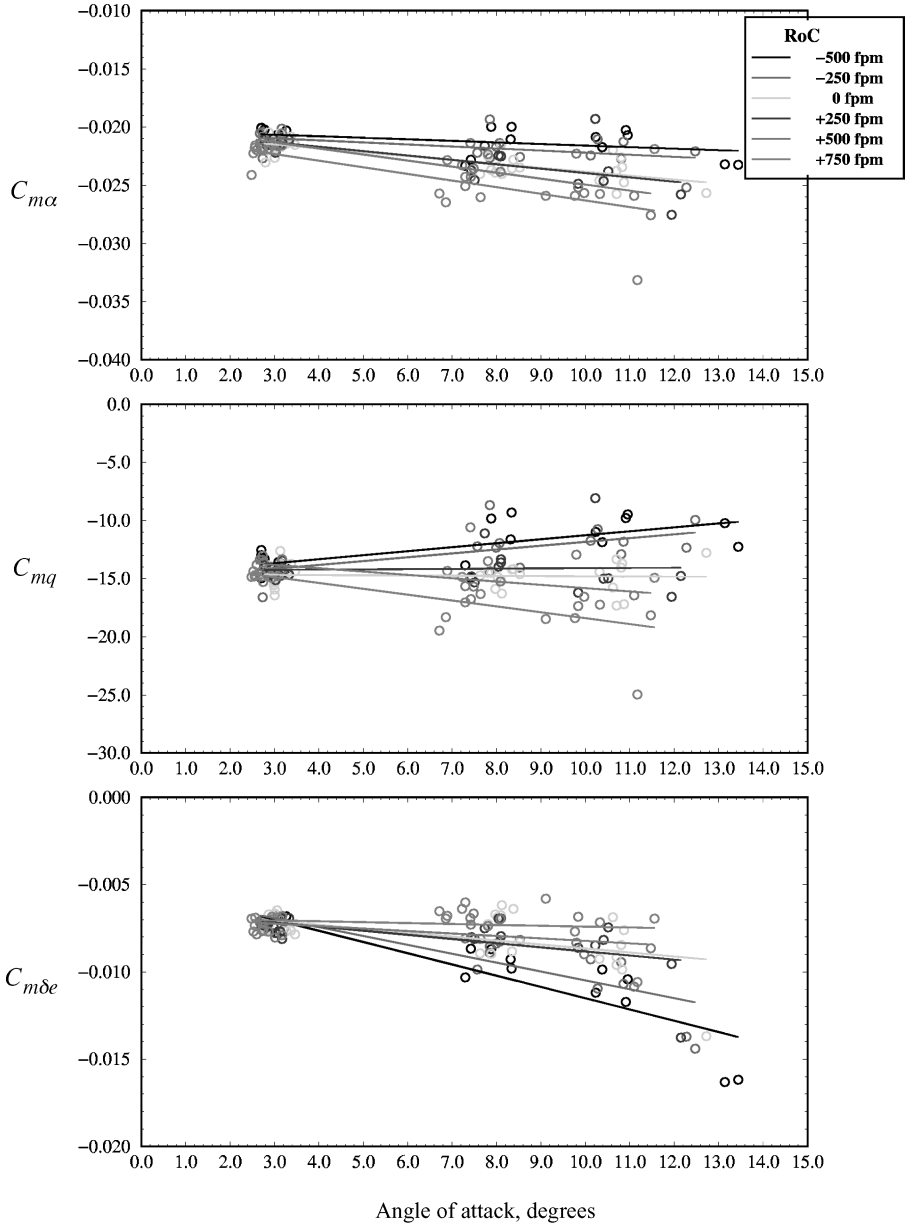

Fig. 13 PC 9/A longitudinal derivative flight estimates at various RoC.

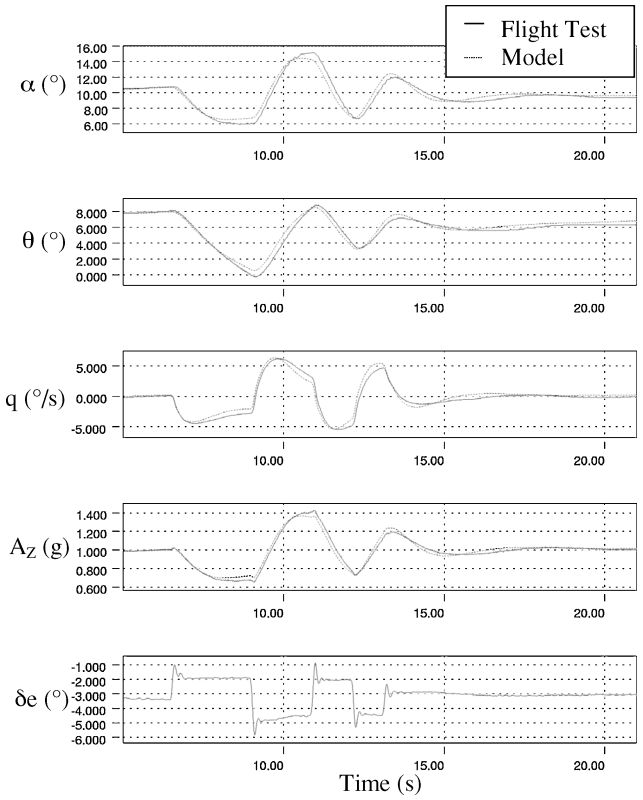

Fig. 14 PC 9/A flight dynamic model response compared with flight test for a sample longitudinal maneuver: $M = 0.2$ and $h = 15{,}000$ ft.

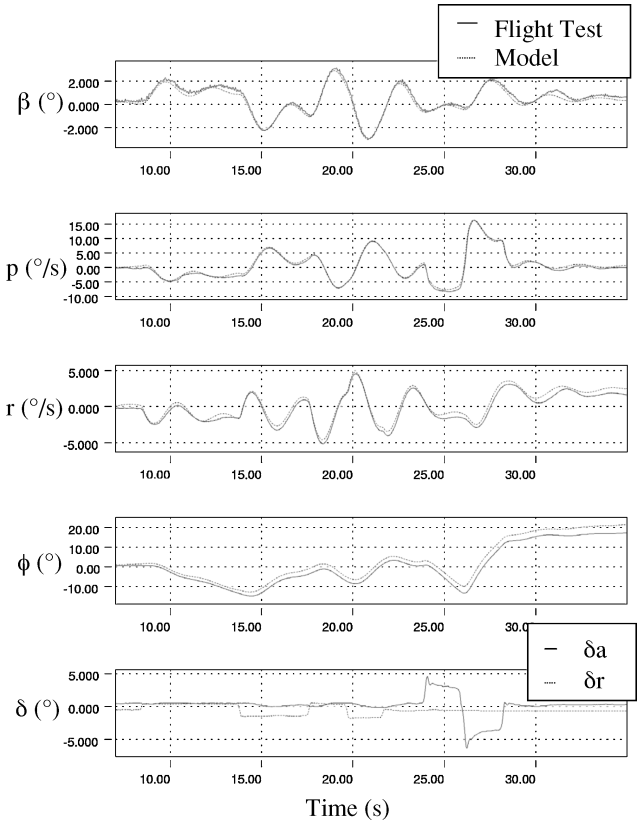

Fig. 15 PC 9/A flight dynamic model response compared with flight test for a sample lateral maneuver: $M = 0.24$ and $h = 5000$ ft.

Power Effects

The 950 SHP turboprop engine exhibits strong power effects on the aircraft handling qualities. To increase the simulator database thrust coefficient and angle-of-attack range, additional flight-test points were conducted. This was investigated by the performance of 3-2-1-1 maneuvers while trimmed, at various rates of climb, from −500 ft/min up to 750 ft/min. Figure 13 presents the results for three stability and control derivatives. Note that the influence of power increases with increasing angle of attack. This is in agreement with theoretical and experimental studies.[12,18] The test points conducted at various rates of climb (RoC) expanded the validation points over a broader thrust coefficient range than possible in steady nonclimbing flight.

PC 9/A Flight Dynamic Model

A flight dynamic model of the PC 9/A aircraft was developed by the use of both flight-test and power-on wind-tunnel aerodynamic estimates. In general, the wind-tunnel data were adjusted with the flight-test estimates following a similar process to that discussed earlier for the F-111C aircraft.

Figures 14 and 15 compare the aircraft flight-measured and open-loop flight dynamic model responses. The longitudinal maneuver consisted of an elevator 3-2-1-1 input. The lateral maneuver consisted of a rudder 3-2-1-1, followed by an aileron doublet input. The measured and simulated responses are in good agreement and are typical of the model's performance throughout the aircraft's operational envelope.

Conclusions

The paper outlines two flight-test programs aimed at the development of flight dynamic models over the flight envelope, rather than at a few points of aerodynamic interest. In both cases, wind-tunnel and other data sources were available a priori.

The F-111C flight-test program results indicated that even with an extensive test matrix, the ability of discrete test data points, coupled with the resultant data being expressed in terms of locally linearized derivatives, results in a data set that has limitations. First, the data is generally not as extensive as a typical wind-tunnel program data set. Second, the nature of system identification techniques, given the vagaries of flight test, does not provide the elegance of wind-tunnel-developed data sets with generally well-defined increments. As a result, difficulties arise when data are matched or compared between flight and more simply controlled ground-based experimental data, such as wind-tunnel data.

The PC 9/A test program again aimed to develop a comprehensive database across the full flight envelope. As stated earlier, the system identification techniques provided an efficient validation data set, but were somewhat more difficult to make use of when an attempt was made to develop a full flight dynamic model across the whole flight envelope. The propeller power effects are accounted for in a more realistic way in flight test. Nevertheless, they are difficult to reconcile with the limited wind-tunnel data thrust coefficient range.

In conclusion, system identification is an efficient technique to provide aerodynamic stability and control databases. They also provide validation data for wind-tunnel or computational data. However, the techniques are expensive in terms of flight-test time if a full matrix of points is required. The resultant sets are more difficult to create at individual angle of attack, sideslip, or Mach combinations as normally required by the aerodynamicist. The methods are complementary and, like wind-tunnel, empirical, and CFD data, they each provide different levels of insight into the aerodynamic behavior. System identification techniques augment the wind tunnel's laboratory-controlled increments without the side effect of the testing methodology such as sting interference, but they do include effects such as those induced by angular rates.

Acknowledgments

The authors wish to acknowledge Colin Martin for his significant input into the F-111C program and the insights provided by Nicholas van Bronswijk regarding the interpretation of the PC 9/A

air brake deployed configuration flight-test results. The authors also wish to acknowledge the help of Bruce Woodyatt, Andrew Snowden, and Hilary Keating from the Defence Science and Technology Organisation.

References

[1]Klein, V., Cobleigh, B., and Noderer, K., "Lateral Aerodynamic Parameters of the X-29 Aircraft Estimated from Flight Data at Moderate to High Angles of Attack," NASA TM-104155, Dec. 1991.

[2]Hamel, P. G., and Jategaonkar, R. V., "Evolution of Flight Vehicle System Identification," *Journal of Aircraft*, Vol. 33, No. 1, 1996, pp. 9–28.

[3]Iliff, K., Maine, R., and Steers, S., "Flight-Determined Stability and Control Coefficients of the F-111A Airplane," NASA TM-72851, March 1978.

[4]Sim, A. G., and Curry, R. E., "Flight-Determined Stability and Control Derivatives for F-111 Tact Research Aircraft," NASA TP-1350, Oct. 1978.

[5]de Souza, C. E., Evans, E. J., and Goodwin, G. C., "Nonlinear Estimation Algorithms for Flight Path Reconstruction," Rept. EE8316, Dept. of Electrical Engineering, Univ. of Newcastle, Newcastle, NSW, Australia, March 1983.

[6]Murray, J., and Maine, R., "pEst Version 2.1 User's Manual," NASA TM-88280, Sept. 1987.

[7]Maine, R. E., and Iliff, K. W., "Application of Parameter Estimation to Aircraft Stability and Control—The Output-Error Approach," NASA Reference Publication 1168, June 1986.

[8]"Manual for the Criteria for the Qualification of Flight Simulators—First Edition," International Civil Aviation Organisation, Montreal, 1995.

[9]"Flight Simulator Design & Performance Data Requirements—5th Edition," International Air Transport Association, Montreal, 1996.

[10]Glaister, M. K., "Low-Speed Wind Tunnel Test on a 17.25% Scale Powered Model of the Pilatus PC 9/A Aircraft," Defence Science and Technology Organisation, DSTO-TR-1134, July 2001.

[11]Astill, S., Woodyatt, B. A., and Bronswijk, N., "A Six Degree-of-Freedom Flight Dynamic Model for the Pilatus PC 9/A," Defence Science and Technology Organisation, DSTO-TR-1108, Feb. 2001.

[12]van Bronswijk, N., "The Effects of Propeller Power on the Stability and Control of a Tractor-Propeller Powered Single-Engine Low-Wing Monoplane," Ph.D. Dissertation, Dept. of Aeronautical Engineering, Univ. of Sydney, Sydney, NSW, Australia, Sept. 2001.

[13]Snowden, A. D., Keating, H. A., van Bronswijk, N., and Drobik, J. S., "A Correlation Between Flight-Determined Longitudinal Derivatives and Ground-Based Data for the Pilatus PC 9/A Training Aircraft in Cruise Configuration," Defence Science and Technology Organisation, DSTO TR-0937, Feb. 2000.

[14]Keating, H. A., van Bronswijk, N., Snowden, A. D., and Drobik, J. S., "A Correlation Between Flight-Determined Lateral Derivatives and Ground-Based Data for the Pilatus PC 9/A Training Aircraft in Cruise Configuration," Defence Science and Technology Organisation, DSTO TR-0988, June 2000.

[15]van Bronswijk, N., Snowden, A. D., Keating, H. A., and Brian, G. J., "A Correlation Between Flight-Determined Longitudinal and Lateral Derivatives and Wind Tunnel Data for the Pilatus PC 9/A Training Aircraft in Approach and Departure Configurations," Defence Science and Technology Organisation, DSTO TR-0479, Nov. 2000.

[16]Williams, J. E., and Vukelich, S. P., "The USAF Stability and Control Digital DATCOM—Volume I, Users Manual," U.S. Air Force Flight Dynamics Lab., Technical Rept. AFFDL-TR-76-45, Nov. 1976.

[17]Williams, J. E., and Vukelich, S. P., "The USAF Stability and Control Digital DATCOM—Volume II, Implementation of DATCOM Methods," U.S. Air Force Flight Dynamics Lab., Technical Rept. AFFDL-TR-76-45, Nov. 1976.

[18]Shivers, J. P., Fink, M. P., and Ware, G. M., "Full-Scale Wind Tunnel Investigation of the Static Longitudinal and Lateral Characteristics of a Light Single-Engine Low-Wing Airplane," NASA TN D-5857, June 1970.